2003-03

A comparison of in-situ measurements and satellite remote sensing of underwater visibility

Museler, Erica A.

Monterey, California. Naval Postgraduate School

NAVAL POSTGRADUATE SCHOOL
Monterey, California

THESIS

A COMPARISON OF IN-SITU MEASUREMENTS AND SATELLITE REMOTE SENSING OF UNDERWATER VISIBILITY

by

Erica A. Museler

March 2003

Thesis Advisor: Philip A. Durkee

Approved for public release; distribution is unlimited.

THIS PAGE INTENTIONALLY LEFT BLANK

REPORT DOCUMENTATION PAGE

Form Approved OMB No. 0704-0188

1. AGENCY USE ONLY *(Leave blank)*	2. REPORT DATE	3. REPORT TYPE AND DATES COVERED
	March 2003	Master's Thesis

4. TITLE AND SUBTITLE
A Comparison of In-situ Measurements and Satellite Remote Sensing of Underwater Visibility

5. FUNDING NUMBERS

6. AUTHOR (S)
Erica A Museler

7. PERFORMING ORGANIZATION NAME(S) AND ADDRESS(ES)
Naval Postgraduate School
Monterey, CA 93943-5000

8. PERFORMING ORGANIZATION REPORT NUMBER

9. SPONSORING / MONITORING AGENCY NAME(S) AND ADDRESS(ES)

10. SPONSORING/MONITORING AGENCY REPORT NUMBER

11. SUPPLEMENTARY NOTES The views expressed in this thesis are those of the author and do not reflect the official policy or position of the U.S. Department of Defense or the U.S. Government.

12a. DISTRIBUTION / AVAILABILITY STATEMENT
Approved for public release; distribution is unlimited.

12b. DISTRIBUTION CODE

13. ABSTRACT ***(maximum 200 words)***

SeaWiFS data converted to optical properties of the ocean in the form of vertical and horizontal underwater visibility products are compared to in-water diver and optical instrument measurements during the Model Diver Visibility (MoDiV) experiment. Results were collected from 19 to 21 August in the Mississippi Bight region of the United States.

The SeaWiFS satellite data was processed with the Automated Processing System (APS), developed by the Naval Research Laboratory (Code 7333). APS converted radiance values into specific parameters studied: the beam attenuation coefficient, the diffuse attenuation coefficient, vertical visibility and horizontal visibility. These values were compared to the AC-9instrument, a-Beta instrument, Secchi disk and the observed visibilities from the divers.

The results indicated that the beam attenuation coefficient and the diffuse attenuation coefficient are underestimated as compared to the in-situ measurements. These values then overestimate the vertical and horizontal visibility as compared to the Secchi disk and diver sightings. The visibility products from SeaWiFS should be used on an experimental basis for Naval Operational Planning. It is recommended that the use of in-water diver reports noting variability of SeaWiFS visibility product estimates are necessary for validation and offers feedback to the research and development field for algorithm improvement.

14. SUBJECT TERMS	15. NUMBER OF PAGES
SeaWiFS, APS, Underwater Visibility	77
	16. PRICE CODE

17. SECURITY CLASSIFICATION OF REPORT	18. SECURITY CLASSIFICATION OF THIS PAGE	19. SECURITY CLASSIFICATION OF ABSTRACT	20. LIMITATION OF ABSTRACT
Unclassified	Unclassified	Unclassified	UL

NSN 7540-01-280-5500 **Standard Form 298 (Rev. 2-89) Prescribed by ANSI Std. 239-18**

THIS PAGE INTENTIONALLY LEFT BLANK

Approved for public release; distribution is unlimited.

A COMPARISON OF IN-SITU MEASUREMENTS AND SATELLITE REMOTE SENSING OF UNDERWATER VISIBILITY

Erica A Museler
Lieutenant, United States Navy
B.S., United States Naval Academy, 1997

Submitted in partial fulfillment of the
requirements for the degree of

MASTER OF SCIENCE IN METEOROLOGY AND PHYSICAL OCEANOGRAPHY

from the

NAVAL POSTGRADUATE SCHOOL
March 2003

Author: Erica A Museler

Approved by: Philip A. Durkee
Thesis Advisor

Robin Tokmakian
Second Reader

Carlyle H. Wash
Chairman, Department of Meteorology

THIS PAGE INTENTIONALLY LEFT BLANK

ABSTRACT

SeaWiFS data converted to optical properties of the ocean in the form of vertical and horizontal underwater visibility products are compared to in-water diver and optical instrument measurements during the Model Diver Visibility (MoDiV) experiment. Results were collected from 19 to 21 August in the Mississippi Bight region of the United States.

The SeaWiFS satellite data was processed with the Automated Processing System (APS), developed by the Naval Research Lab (Code 7333). APS converted radiance values into specific parameters studied: the beam attenuation coefficient, the diffuse attenuation coefficient, vertical visibility and horizontal visibility. These values were compared to the AC-9 instrument, a-Beta instrument, Secchi disk and the observed measurements from the divers.

The results indicated that the beam attenuation coefficient and the diffuse attenuation coefficient are underestimated as compared to the in-situ measurements. These values then overestimate the vertical and horizontal visibility as compared to the Secchi disk and diver sightings. The visibility products from SeaWiFS should be used on an experimental basis for Naval operational planning. It is recommended that the use of in-water diver reports noting variability of SeaWiFS visibility product estimates are necessary for validation and offers feedback to the research and development field for algorithm improvement.

THIS PAGE INTENTIONALLY LEFT BLANK

TABLE OF CONTENTS

LIST OF FIGURES

LIST OF TABLES

THIS PAGE INTENTIONALLY LEFT BLANK

ACKNOWLEDGEMENTS

I would like to thank my advisor, Dr. Philip A. Durkee of the Department of Meteorology, Naval Postgraduate School, for his patient guidance and support during the development of this thesis. Additionally I would like to thank Robin Tokmakian for input as second reader and Kurt Neilsen for his programming and processing assistance.

I would also like to extend my utmost appreciate to the Ocean Color team at the Naval Research Laboratory, Stennis Space center: Bob Arnone, Alan Weidemann, Paul Martinoloch, Wesley Goode, Ricky Ray, and The Naval Oceanographic Office Dive Team. Without their willingness to nurture my endeavor, I would not have had the opportunity to pursue this topic.

Finally, my heartfelt appreciation goes to my Mother, Father and Opa for their intellectual encouragement, and constant support without which I would not have had the motivation or creativeness to complete my work. I dedicate this thesis and my degree to them with all my love.

THIS PAGE INTENTIONALLY LEFT BLANK

I. INTRODUCTION

In today's War on Terror our military has the urgent and continuous need for accurate, timely and detailed environmental data to support field operators/warriors. The focus of this thesis is operational remote sensing of ocean optical parameters related to underwater visibility in support of the Mine Warfare (MW) and Special Warfare (SPECWAR) communities. Remotely sensed (RS) information provides the pertinent optical properties of the ocean that help in operational planning and in tactical decision-making. An enormous benefit to RS oceanographic information is the ability to access data from otherwise restricted waters. The Naval Research Laboratory (NRL) at Stennis Space Center (SSC) provides such detailed data pertaining to the ocean's optical properties and underwater visibility. Utilizing the information downloaded from the Sea Viewing Wide Field of View Sensor (SeaWiFS) on the OrbView-2 Satellite, the Automated Processing System (APS), NRL code 7333 (Ocean Optics Section of NRL) produces images of oceanographic optical parameters. When interpreted, these satellite images can greatly assist Naval leaders in planning as well as give the operator prior knowledge of the conditions of their environment.

Inherent to all Naval Operations is the need for the warfighter to exploit their environment for tactical advantage and quick strike capability. With RS environmental imagery and information, today's warfighter has the distinct advantage of knowing detailed information in otherwise restricted areas prior to a mission.

Exploiting the operational environment has always been critical to the success of military missions. The Strategic Plan of the Naval Meteorology and Oceanography community includes the need to define virtually any operating environment to on-scene, tactical forces.

A. HISTORY

The Navy's involvement with research in ocean optics spans nearly 50 years. The academic science and research communities, NRL, and the Navy's own METOC corps has greatly contributed to the Navy's ocean optical advances in underwater visibility that supports various warfare communities.

A report for the Department of the Navy funded by the Office of Naval Research in November 1968 resulted in ocean optical theories that are still being used by the Navy today. Williams (1968) solidifies the use of the white Secchi disk and it's ability to extract the inherent water parameters of beam attenuation and extinction. The Secchi disk is the simplest and least expensive measure of water visibility. The report stated that to make accurate measurements of visibility the disk should be combined with results of in-situ measurements from other optical measuring instruments.

Other subsequent papers and textbooks in the civilian realm of ocean optical research have concluded the importance of proper Secchi disk measurements integrated with modern instruments that can ultimately measure beam attenuation with depth in turbid water. Holmes (1970) clearly states that in turbid waters and in the green region of the spectrum a "statistically significant"

relationship exists between the secchi depth and light transmission thru the water.

Nomographic charts were developed in the late 1950s and 1960s for sighting ranges given target and view angle, and also other environmental parameters. Extrapolating atmospheric light attenuation and range to the ocean developed the basic principle of the sighting range. Target contrast parameters for underwater scenarios are often unknown. Therefore it is difficult to predict the range at which a possible threat may be seen since specific parameters of the target are uncertain.

Today, the Navy attempts 'Through The Sensor' technology by utilizing forward deployed ships, unmanned autonomous vehicles (UAVs) and diver inputs for direct measurement of inherent optical properties. These measurements directly benefit research and operational interpretation of RS data in understanding and exploiting the ocean environment.

B. MOTIVATION

A majority of politically sensitive countries have ocean borders resulting in denied access to critical areas. Knowledge of ocean parameters in these areas require RS retrievals or modeled properties. SeaWiFS's global coverage provides information for these regions and, together with APS products, arm the METOC officer with crucial environmental information. This offers an advantage in support of communities utilizing ocean data for operational planning and execution.

Two communities that have a constant use for ocean optical properties are MW and SPECOPS. With the help of

the National Research Council, each community has been able to hold a symposium between scientists and operators to convert experimental/research products to real-time operational products.

The National Research Council (2000) sponsored and published a symposium between oceanographic researchers and Naval Warfighters in the MW community. Together they identified numerous areas where science and technology that could strengthen the Navy's Mine Warfare capabilities if implemented and exploited. In particular, optical properties of the water are of great importance to both ship sensors and to human divers who operate in that medium. The ability to see well enough to detect, classify and neutralize floating and hull mounted mines is imperative. A diver knowing the conditions of the water before entering has a tactical environmental advantage. The operational planner who knows in advance that the visibility in the search area is poor may choose to send a dolphin or sea lion, which can easily locate a mine, vice a human, saving time in the overall mission of neutralizing a threat.

The National Research Council (1997) also sponsored and published a symposium that brought to light many facets of ocean optical properties that are significant to mission-critical environmental parameters for SPECWAR. In the Naval Special Warfare (NSW) Mission Planning guide, swimmers or Seal Delivery Vehicles (SDVs) should not operate in water that allows them to be observed at distances greater than 10 feet. Although this restriction is placed on the warfighter, turbid water can also impede

the navigation of the mission causing a decrease in underwater line of sight and ability to see dive meters or navigational aids. Also realized in the symposium was the capability of underwater vehicles, such as the SDVs, that can support the housing of small instruments to collect optical and hydrological data. Demonstrations of underwater autonomous vehicles (UAVs) for tactical collection of optical data are forthcoming this next year. Hydrological data collected and returned to the METOC centers can be archived for oceanographic handbooks. This data should also be submitted to the research community.

Presently a basic model of visibility for these communities is available via SeaWiFS and APS. Because many times the target is unknown, the vertical clarity of the water or the horizontal visual range of the human eye are the only tools that provide the environmental advantage to the warfighter. Some limitations to the near real-time aspect of satellite remote sensing are cloud cover, atmospheric aerosols and the near surface limitation such as near shore white caps. These disturbances distort the radiance received by the SeaWiFS sensor.

THIS PAGE INTENTIONALLY LEFT BLANK

II. THEORY

Hydrologic optics is closely associated with atmospheric radiative transfer theory but applied to the ocean medium. Radiative transfer theory is defined as the quantitative study, on a phenomenological level, of the transfer of radiant energy through media that absorbs, scatters or emits radiant energy (Preisendorfer 1976). Radiant energy from the sun is transferred in an array of wavelengths in the form of electromagnetic energy. The part of the energy spectrum detected by humans by sight is the visible wavelengths, 390 to 740 nanometer (nm) wavelengths. Peak brightness to the human eye is measured at approximately 555 nm under normal daylight conditions but changes with low light adaptation. The ocean interface introduces modifications to the radiative transfer process; a smooth water surface immediately reflects approximately 2% of the incoming electromagnetic energy while transmitting approximately 98% of that energy through its medium. Transmission of this energy is also dependent of the angle of incidence. When the ocean surface becomes roughened by wind and waves the reflection and transmission pattern becomes much more complex.

Preisendorfer (1976) presents a simple model for radiative transfer:

$$\frac{dL}{dr} = -(a+b)L + L_{*}, \qquad (1)$$

where L is the apparent radiance, r is the path distance, a being absorption, b is backscattering, and L_{*} is the path

function that includes the amount of radiance scattered without a change in wavelength. Equation (1) holds for all visible wavelengths. Along that path a series of scattering (b) and absorption (a) modify the transfer of radiation. The combination of absorption and scattering is commonly referred to as the beam attenuation coefficient, c where $c = a + b$. There are also photons that are neither scattered or absorbed and travel the entire path length.

Knowing the beam attenuation coefficient and path function equation (1) can now be represented over the entire path length through integration. Scattered visible light in the ocean also decreases exponentially with depth. This model connects the radiance at the beginning and end of an arbitrary radiance path:

$$L(r,\theta) = L_0(r,\theta)e^{-cr} + \int_0^r L_*(r',\theta)e^{-c(r-r')}dr \quad , \qquad (2)$$

For visibility θ represents the view angle of the human. In this thesis the coordinate system is oriented such that when a diver is looking up at the surface of the water $\theta = 0^o$.

The final simple model for radiance is the synthesis of equations (1) and the assumption of light's exponential attenuation in the water:

$$L\ (r,\theta) = L_o(r_o,\theta)e^{-cr} + \frac{L_*(r,\theta)}{c + K\cos\theta}[1 - e^{-(c+K\cos\theta)r}] \quad , \qquad (3)$$

This equation does not include the dependence on the azimuth angle or location of the sun. For the purposes of this thesis the angle of the sun will be directly over-

head, providing a sufficient background light field.

Equation (3) can be simplified even further to basic rules of contrast theory to also include the problem of the attenuation of light while viewing an object. To be seen by the human eye an object must have a minimum contrast with its surroundings. Brightness contrast is defined as:

$$C_o = \frac{L_T - L_B}{L_B} \quad , \tag{4}$$

where (L_T) is the object (target) radiance or brightness and (L_B) is the background field radiance. To be seen by the human eye an object must have a minimum contrast with it's surroundings usually taken to be –2%. In the same fashion that light is affected by water, contrast is also attenuated exponentially with depth. The combination of equation (3) and (4) results in this equation:

$$C_r = C_o e^{[-(c+K\cos\theta)r]} \quad , \tag{5}$$

with C_r as the apparent contrast. This equation can be used to solve for visibility lengths represented by r. The clarity of natural waters can be expressed directly in terms of the beam (c) and diffuse (K) attenuation coefficient. A variety of instruments can measure c and K as well as the absorption and scattering quality of natural waters. Solving for r in equation (5):

$$r = \frac{-\ln(\frac{C_r}{C_o})}{c + K\cos\theta} \quad , \tag{6}$$

The simplest assumption for the contrast ratio is using a blackbody target with a known inherent contrast of –1, and with a sufficient light field the background contrast is approximately equal to –0.02. This simplifies the numerator in equation (6) to approximately 4.0. Different contrast values have been established thru empirical and studied calculations in various types of water. When viewed vertically, with θ=0^{o}, the range equation is reduced to:

$$r_{vertical} = \frac{4.0}{c + K}, \qquad (7)$$

The horizontal range is viewed with θ=90^{o} and is represented by:

$$r_{horizontal} = \frac{4.8}{c}, \qquad (8)$$

The 4.8 contrast value was derived from previous contrast comparisons performed at NRL using a variety of targets. Equation (7) and (8) are the algorithms used by SeaWiFS to represent the vertical and horizontal visibility products.

The contrasts values in the numerators of equation (7) and (8) are not universal and depend on the object's size, angle viewed by the swimmer, object reflectance and angle of the sun in the sky. In this thesis these dependent parameters were simplified to assume that the object size was unknown, the angle viewed by the swimmer was vertical or horizontal, the objects reflectance was considered as a black body and the sun was overhead at solar noon providing a well-lighted background field.

A. INHERENT AND APPARENT OCEAN OPTICAL PROPERTIES

Inherent to the water medium are the properties of the volume attenuation function (c) that includes the sum of scattered (b) and absorbed (a) energy and the volume scattering function. Some energy that enters the water medium is neither scattered nor absorbed and transmits with no change.

Apparent optical properties are those dependent on the light field. This field is determined by the nature of the incident light in the ocean medium and the inherent optical properties of that medium. The diffuse attenuation coefficient K is defined in terms of the exponential decay of the ambient irradiance with depth. The directional structure of the light field, the sun in this case, is directly related to the parameter K as is the ratio of the scattering to total attenuation.

1. The Remote Sensing of Optical Properties

The intensity of light in the ocean influences the biological processes that result in light becoming scattered and absorbed. Figure (1) illustrates the interaction of the energy from the sun with the ocean, absorption by water, particles and colored dissolved organic material (CDOM). Backscattering occurs due to the water and from both inorganic particles (sediment), and organic (phytoplankton) particles. The satellite receives the water leaving radiances after is has been effected by these ocean processes. Molecular and aerosol scattering typically allow 10-30% direct transmittance of the water leaving radiance to the satellite. Correction of the atmospheric effects is derived from analysis of the red and

near-infrared radiance that are not affected by ocean properties.

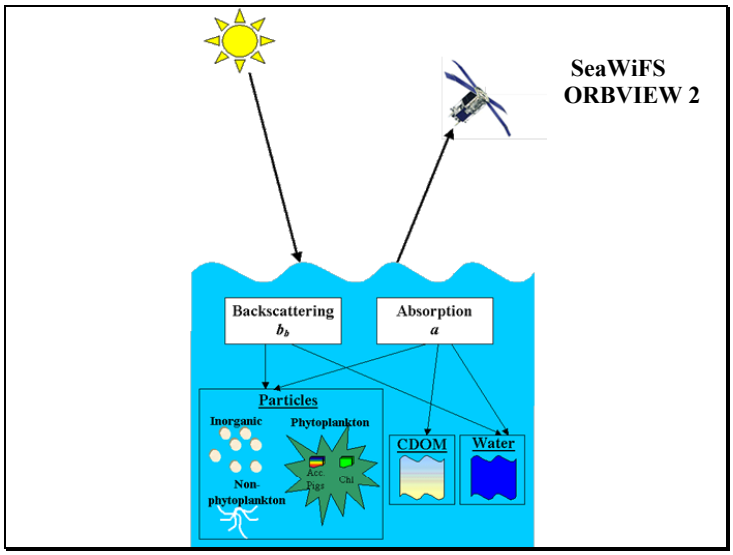

Figure 1: Interaction of solar radiation with the ocean and the received radiance to the satellite. http://www.bigelow.org/~ahb/gomoosopticalweb/Ocean_optics/oceanoptics.htm (8/23/2002)

In a simple diagram, as in figure (2), the summary of the remotely sensed reflectance as seen by the satellite starts with the radiances from the sun and sky. Important to remotely sensed surface parameters is the radiative transfer of the suns energy through the sky. The reaction of the energy from the sun on the ocean causes biological productivity to increase, changing the influence of suspended material in the ocean on both the inherent and apparent optical property parameters. Light in the water column that has been redirected upward is observed by SeaWiFS. The ratio of upwelling radiance to down-welling radiance (light from the sun to the ocean) is directly related to inherent optical properties of the ocean.

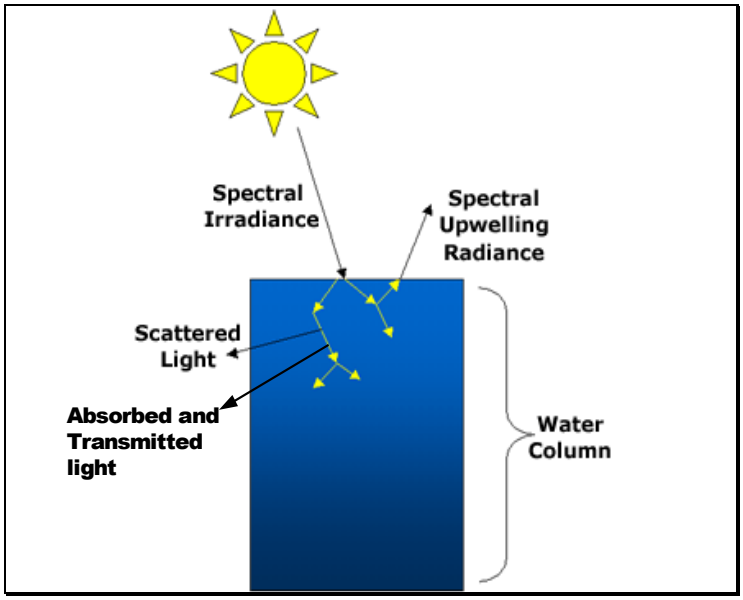

Figure 2: Sunlight incident on the ocean surface and the redirected upwelling light produced from the reaction of scattering and absorption by the water. http://www.bigelow.org/~ahb/gomoosopticalweb/Ocean_optics/oceanoptics.htm (8/23/2002)

SeaWiFS receives the reflected light at all wavelengths. The ocean absorbs red wavelengths in 8 wavelength bands. The ocean absorbs red wavelengths in the visible portion of the spectrum, which is why natural waters appear blue. The wavelengths pertinent to horizontal and vertical visibility are in the green wavelengths, 532 and 555 nm. A plot of the spectral distribution of the sun at the sea surface, Williams (1968) observes also that the human eye is “strongly peaked at the 555 nm wavelength”.

After Zaneveld (1994), figure (3) presents a flow chart for the relationship of RS from the sun to the sensor and finally to the interpreter of the product. The final portion of processing the received reflectances of SeaWiFS is the APS conversion of the radiance received and the METOC interpretation of the satellite information. APS is a powerful tool that incorporates the physical theories of

underwater optics. By understanding the basic oceanographic optical property concepts above, and also being familiar with the APS tool, the METOC officer can now establish a baseline report for the optical conditions of the operational area of the day.

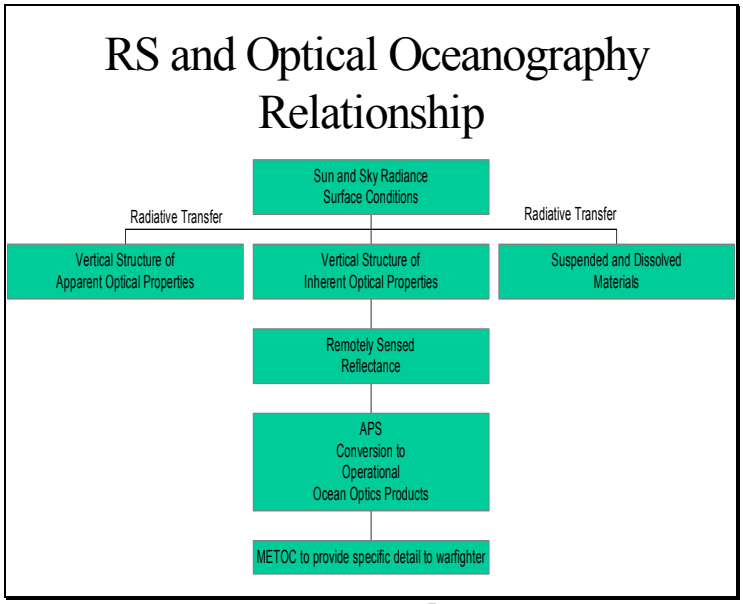

Figure 3. After Zaneveld (1994), sun to sensor to interpreter flow chart for RS optical products.

III. DATA

A. IN SITU MEASUREMENTS

Measurements of ocean optical parameters were collected from 19 to 23 August 2002, during the Model Diver (MoDiv) experiment in the Mississippi Bight region of the Gulf of Mexico ($30^{\circ}5.5'N, 88^{\circ}52.5'W$). A series of dives were conducted with simultaneous measurements using various optical instruments from approximately 1100 to 1500 Local Time (LT) each day. The time of day was planned to match with SeaWiFS overpasses and to maximize the sun's illumination at or near solar noon. The primary objective of the experiment was to compare the visibility models represented by equations (7) and (8). These equations are the APS algorithms for horizontal and vertical water visibility.

The MoDiv field experiment was conducted to determine how well each model performed and to compare the parameters derived from the Secchi measurements to the SeaWiFS products from APS. The MoDiv exercise plan (Jugan, 2002) contains details of the field collection effort. The experiment data covers three days of in situ and satellite ocean optical measurements. This thesis uses the models from equation (7) and (8) to compare in-situ measurements and diver observations to the SeaWiFS derived measurements in order to assess their operational utility.

1. Instruments

Instruments were deployed from the ship platform using a low-decent rate ocean profiler. The following instrumentation was included: AC-9 plus, a-beta, c-beta,

Conductivity Temperature and Density Sensor, ECO Volume Scattering Function (ECO-VSF), Hyperspectral Tethered Spectral Radiometer Buoy (Hyper-TSRB), Tethered Attenuation Coefficient Chain Sensor (TACCS k-chain), white Secchi disk and a multiple wavelength backscattering sensor (Hydro-Optics, Biology & Instrumentation (HOBI) labs Hydroscatt). Lab calibration required for instruments was done prior to field deployment. The following sections will briefly describe each instrument's measurement as they pertain to the subject of horizontal and vertical visibility. (Table 1 provides a brief review of the instruments and measurements used to define optical properties for horizontal and vertical visibility.)

a. AC-9 Plus

The AC-9 Plus performs concurrent measurements of the water's total attenuation (c) and absorption (a) characteristics by utilizing a dual path configuration in one instrument. Each path contains its own light source, optics and detectors for the specific wavelength measurement. The instrument used wavelengths from 412 nm to 715 nm.

b. a-Beta and c-Beta

The a-beta and c-beta both measure backscattering. A source light travels through an internal prism that bends the beam before it enters the water; the receiver has a similar prism that bends the field of view towards the source beam. The source beam divergences, the prism angles, and distance between the source and receiver windows determine the range of scattering angles over which the measurement is made. Both instruments provide

measurements centered on a scattering angle of 140° at 532 nm.

The c-Beta instrument also measures (c) through a folded-path beam transmissometer. The round trip distance of the incident beam of light travels through a 30 cm glass housing. Any light scattered out of the beam over that path length contributes to the measured attenuation.

The a-Beta instrument measures the returned radiance over a round-trip path length of 30 cm. In contrast to the c-Beta, the geometry provides a measurement of diffuse attenuation (K) that is affected by wide-angle scattering and absorption. The effect of wide-angle scattering can also be determined empirically from the backscattering measurement, and then subtracted from the K measurement to provide an accurate estimate of absorption.

c. Conductivity-Temperature and Depth Profiler (CTD)

The CTD measures three parameters directly: conductivity, temperature and pressure. Salinity is estimated from the waters conductivity of electric currents that pass through salty water. Water that has a higher salinity passes more current than brackish or fresh waters. A thermister measures the temperature and a quartz crystal-based gauge measures pressure throughout the water column.

d. ECO-Volume Scattering Function (VSF)

The ECO-VSF measures optical scattering at three distinct angles: 100, 125 and 150 degrees, at three wavelengths (450, 530 and 650 nm) thus providing the shape of the volume scattering function. The three-angle measurement allows determination of scattering at specific

angles through interpolation. Conversely, it also may provide the total backscattering coefficient by integration and extrapolation from 90 to 180 degrees.

e. Hyper-TSRB

This instrument contains two high-quality 256-channel spectrographs that obtain hyperspectral measurements of upwelling radiance and downwelling irradiance. This data can be used with the TACCS (see next instrument) to calculate remote sensing reflectance. The Hyper-TSRB is designed to obtain upwelling near surface spectral radiance data at sub-wave period sampling rates away from the observing platform disturbances.

f. TACCS k-Chain

The TACCS system is designed to allow the user to obtain the instantaneous diffuse attenuation coefficient of the water column without performing optical profiles. The k-chain is attached to the TSRB to accurately determine the diffuse attenuation in the optical light field. The chain has 6 sensors located at depths of 1.5, 1.75, 2, 2.25, 2.5 and 2.75 meters in order to calculate K. These are cosine irradiance sensors at the 532 nm wavelength.

g. White Secchi Disk

The Secchi disk is the oldest instrument used to decipher the clarity/visibility of the water in the vertical coordinate system. It is a simple instrument, yields immediate information regarding the water clarity and its cost is significantly less than spectral measuring instruments. A 12 inch white disk is lowered into the water and the depth at which the white disk disappears is the secchi depth. Combined with the more expensive

instruments the secchi results yield multiple optical properties of the ocean such as: c, and K. The white disk was used in the MoDiV experiment. The use of a black disk presents an easier assumption in using contrast theory for water clarity but was not used in the experiment for vertical visibility.

h. HOBI Labs Hydroscatt

The Hydroscatt is a self-contained instrument that measures optical backscattering (b_b) at six different wavelengths, and fluorescence. The source produces a beam of light in the water and the detector collects a portion of the light that is scattered out of that beam by the water. The divergence of the source beam and receiver field of view, the angle of the prisms, and the distance between the source and receiver windows, determine the range of the scattering angles measured. The Hydroscatt geometry results in a measurement centered on a scattering angle of 140°. Its backscattering sensor is nearly identical to that of the a-Beta and c-Beta (same manufacturing company).

i. SeaWiFS Sensor

The SeaWiFS sensor measures the sunlight reflected off particulate matter suspended in the water is as water leaving radiance (L_w). Approximately 15 pole-to-pole orbital swaths are completed resulting in approximately 90% of the ocean surface being scanned in two days. SeaWiFS is a spectroradiometer that measures the return radiance at 8 different visible/near infrared (IR) wavelengths. This passive sensor utilizes 8 spectral bands in the visible and near-infrared wavelengths. The eight

bands and wavelengths are as follows: Band 1 - 412 nm (violet), Band 2 - 443 nm (blue), Band 3 – 490 nm (blue-green), Band 4 – 510 nm (blue-green), Band 5 – 555 nm (green), Band 6 – 670 nm (red), Band 7 – 765 nm (near IR) and Band 8 – 865 nm (near IR). The advantage of the space-based spectroradiometer is global coverage while the disadvantage is that interfering optical effects of the aerosol (clouds), sea surface (sea foam). Spatial variability must be accounted for to provide an accurate measurement of L_w relative to in situ validation of measurements.

The water leaving radiances measured are applied to algorithms that produce geophysical values for ocean color studies. These algorithms are tested against highly accurate measurements of radiances at the surface of the ocean as well as immersed in the ocean to measure both the incoming (downwelling) and outgoing (upwelling) radiation. Geophysical values include chlorophyll concentration (Chl), absorption (a), backscattering (b_b), beam attenuation (c) and diffuse attenuation (K_d). SeaWiFS local area resolution is 1 km. The spatial variability of the geophysical phenomena may not be resolved by the satellite resolution. Ocean visibility is particularly variable within 1 km. However, the visibility product provided from SeaWiFS by APS offers resolution to the coastal visibility area of interest in this thesis.

j. Underwater Camera (Diver's Eye)

Four divers estimated the horizontal visibility of the black and gray spherical targets and black disk. Prior to the experiment the divers took an eye test. This

eye test simply proved that each observer was eligible for sighting the underwater targets. For the average Navy Diver or SEAL eye underwater it is assumed that they are fully familiar with the underwater environment, well acquainted with the objects for which they are looking and possess perfect vision within Navy Standards. It is also assumed that the diver knows the direction in which to look and see the visual target. Note also that unexpected targets will be less well detected initially than will those whose appearance will be anticipated. Each diver approached the target from a north, south, east and west direction. The prevailing visibility for that day was an average of all the sightings from the divers including every angle of the two targets.

Table 1: Summary of instruments and measurements of optical properties for horizontal and vertical visibility.

	Instrument	Deployment Method	Measurements	Units
1	ac-9	Vessel	a, c	1/m, 1/m
2	a/c-Beta	Vessel	a, c, $K_{(derived)}$	1/m, 1/m, 1/m
3	CTD	Vessel	S, T, d	ppt, ^{o}C, m
4	ECO-VSF	Vessel	b_b	1/m
5	HTSRB	Vessel	R_d, L_u, R_s	1/sr, W/m^2, 1/sr
6	K-chain	Buoy	K_d	1/m
7	Secchi Disk	Vessel	Vertical Visibility	m
8	Hydroscatt	Vessel	b_b	1/m
9	SeaWiFS	Space Vehicle	K_d, a, b_b	1/m, 1/m, 1/m
10	Underwater Camera	Diver	Horizontal Visibility	m

B. SATELLITE SOFTWARE: AUTOMATED PROCESSING SYSTEM (APS)

APS is a collection of computer programs and shell scripts designed to automatically generate map-projected image databases of satellite derived products from a large volume of raw satellite input. APS provides for near real-time processing with the option of reprocessing historical data from Advanced Very High Resolution Radiometer (AVHRR), SeaWiFS, Modular Optoelectronic Scanner (MOS) and Moderate-resolution Imaging Spectroadiometer (MODIS) sensors. APS version 2.6 incorporates the processing algorithms employed at the Naval Research Laboratory as of October 1 2002. APS is capable of running on the Red Hat Linux 7.1 or SGI IRIX 6.5 operating systems. Currently at NPS, APS 2.6 is configured for reprocessing historical data for research and teaching purposes within the METOC Remote Sensing Laboratory.

Individual scenes are sequentially processed from the level-1 raw digital counts using standard parameters to radiometrically and geometrically correct products to level-3 within several minutes. Level-3 regional data products from APS contain atmospherically corrected geophysical products in standard map projection (Mercator) for a specific region of interest from SeaWiFS. One quick feature of APS is the generation of browse images. As data is being processed (or reprocessed) the browse images are generated allowing the user to instantaneously see the image and concurrently process RS data. Figure 4 is an example of a level-3 browse image for SeaWiFS horizontal visibility August 20 2002. The image clearly shows an

accurate coastline of the Mississippi bight region in a Mercator projection. The image also shows a color bar that defines a general estimate of the horizontal visibility at a given location. Here the higher horizontal visibility areas are represented in blue and the lower visibility areas are in the red-orange colors.

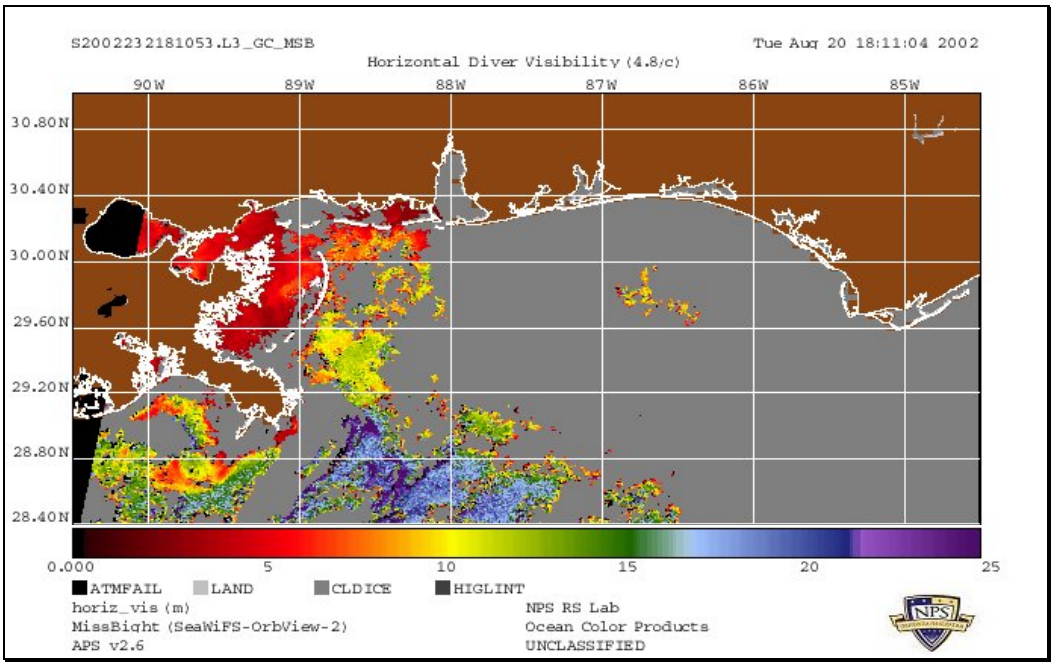

Figure 4: APS level-3 browse image for horizontal visibility August 20, 2002.

Map areas can be created for any portion of the earth. APS will systematically search the level-1A files that match the area mapped and apply the satellite data to the projection. Area maps should be created knowing the resolution limits of the sensor. SeaWiFS provides global resolution of 4 km and local resolution of 1 km, therefore the created maps should remain in these limits for best resolution of the desired parameters.

APS further processes the data into daily, weekly, monthly and yearly temporal composites, which defines level-4 products. There are also hierarchical data format (HDF) files for level-3 and level-4 analysis. HDF files can be used for further manipulation and study in other image software packages such as Environment for Visualizing Images (ENVI) and SeaWiFS Data Analysis System (SeaDAS). Figure 5 shows the HDF horizontal visibility file as viewed using SEADAS on 20 August 2002. The user can define a land mask and a color bar to view and enhance product results. Notice the geo-referenced image has a different projection and a color scheme that is opposite to the APS browse image. SEADAS does allow the user to locate a specific geographical location with a mouse cursor and extract product values. A predefined color scheme of 'rainbow' was used to create this image. The higher horizontal visibility areas are in red and the lower visibility areas are in blue.

Due to cloud coverage throughout the three-day MoDiV experiment the amount of useable data is less than desired. However, the necessary measurements for the determination of a gross detection model under sufficient light and an average eye are attainable. Simplifying the model with the assumption of inherent and apparent contrasts and eye detection limits also allows good use of this limited data.

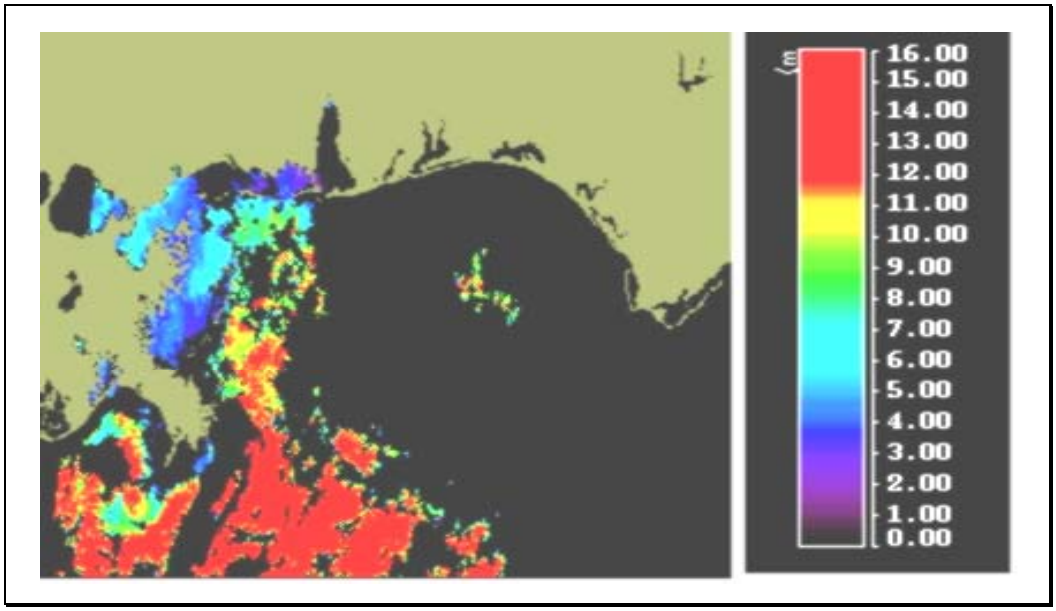

Figure 5: HDF file from APS utilized in SEADAS for manipulation and enhancement. Image is from 20 August 2002 of horizontal visibility with a color bar that can be produced and altered by the user. Cursor location of a particular Lat/Lon provides geo-referenced values.

THIS PAGE INTENTIONALLY LEFT BLANK

IV. PROCEDURES

A. SATELLITE DATA COLLECTION, PROCESSING, AND SCREENING

Preliminary investigations of atmospheric clarity are necessary to determine the effects of the atmosphere on satellite received ocean radiance. The aerosol optical thickness (AOT) for the area of interest was taken from the Aerosol Robotic Network (AERONET) site located at Stennis Space Center. AERONET measures aerosol optical properties using a CIMEL sunphotometer at surface sites located around the world.

SeaWiFS data sets are obtained with the permission of the SeaWiFS Project at the Goddard Space Flight Center (GSFC). The Goddard Earth Sciences Distributed Active Archive Center (GESDAAC) provides access to global satellite data. The files are initially in a level-1A HDF zipped format.

Once the level-1A data is successfully transferred to the NPS RS Lab's Linux computer via File Transfer Protocol (FTP), APS can process the data for ocean optics analysis. A multitude of processing products is available thru APS and can be found in the Data Product User's Guide for APS. The following products were produced for this study:

- c at the 555 nm wavelength using Carder and Arnone's algorithms,
- Chlorophyll-a using the OC4 algorithm,
- Horizontal visibility,
- vertical visibility,

- K at the 532 nm wavelength and
- true color.

Level-3 (direct reprocessing of the individual passes for the given parameters) and Level-4 (composite images for daily, 8-Day, weekly, monthly and yearly) files were created in both the browse format as well as in HDF for geo-referenced values.

The OC4 algorithm for determining Chlorophyll-a concentrations is dependent on the optical properties of the waters being observed. It is an empirical algorithm based on more than 2800 bio-optical in situ measurements of Chlorophyll-a from all over the world. The algorithm uses 4 spectral bands from SeaWiFS for this calculation and was established by the SeaWiFS Project and Calibration and Validation Team. This parameter was not specifically compared in this thesis but offers a quick idea of the clarity of the water regarding phytoplankton blooms excluding non-organic material such as suspended sediment.

The “K532” product from NRL represents the rate at which light at 532 nm is attenuated with depth. Typically the attenuation length is similar to the Secchi depth (bulk measurement) and can be used to estimate the depth, which you can see into the water column. The browse image allows the user to quickly notice large-scale ocean optical features. For each browse file there is a subsequent HDF file with attributes specific to the processed file and defined parameter. The HDF file when viewed in SeaWiFS Data Analysis System (SeaDAS) can pin point exact latitude and longitude location values for the parameter of interest for a particular satellite pass. This allows for a direct

comparison with the data collected and observed in the ocean at that same location and approximate time as the satellite overpass.

Geo-referenced data from each pass was recorded using SEADAS. An Area of Interest (AOI) or the 'blotch' function on SEADAS was created to statistically evaluate the pixel data produced for the region surrounding the experiment's location. Because each individual pass did not render a value for the specific location of the MoDiV experiment, statistical information to include the mean and standard deviation was used to characterize the satellite values. The individual satellite pass for 20 August 2002 yielded the clearest area for study of measurements conducted simultaneously at the MoDiV experiment location. The results presented will include the satellite data from that day.

When the individual pass excluded values for the AOI, then the next step was to examine the daily then weekly composite images. Compilation of data (daily and weekly level-4 files) produced an average value for all products listed for the level-3 files. It should be noted that compiling images compounds any possible error associated with each product. The difference between the three-day visibility average and the composite visibility is large. Because of this fact, the results of a daily and weekly composite are only shown for horizontal visibility.

B. IN SITU DATA COMPILATTION, ORGANIZATION & COMPARISON

A determination of the best instrument to measure the beam and diffuse attenuation coefficients in the water column was established for comparison with the diver and

satellite measurements. Each day, two profiles of the optical properties of the water column were obtained at the time of the satellite pass. Each profile was organized into a 'super sheet' that included the AC-9, a-Beta and c-Beta wavelength measurements with depth. All values were averaged over a depth of 3 meters to directly compare to the depth at which the divers were sighting the targets. The targets consisted of 20-inch black and gray spheres as well as a flat black disk. The spherical targets were made to simulate possible shapes and colors that a Navy diver or swimmer might expect to encounter underwater. The black disk has a theoretical advantage because its contrast ratio is –1, which an easier assumption for calculation using the horizontal and vertical visibility models from SeaWiFS. In this experiment a white Secchi disk was used to determine the in-situ vertical visibility.

The wavelengths measured in the Modeling Diver Visibility (MoDiV) experiment for a validation of present modeling efforts ranged from 443 to 773 nm wavelengths. For the focus of this thesis the 532 and 555 nm wavelengths are used. Because of the natural properties of turbid water, use of the green portion of the visible spectrum is essential. Also, the SeaWiFS green band is centered at the 555 nm wavelength, making 555 nm the preferred wavelength to study optical property measurements. Plots of the c parameter measured by the AC-9 and c-Beta in the 532 and 555 nm wavelengths reveal no significant differences within an average depth of 4.6 meters over the three days studied. Beyond this depth the c-Beta shows considerable difference compared to the AC-9. For this reason, the AC-9 was chosen to represent the inherent optical properties of the water

for comparison. Chapter V will further support the AC-9 and c-Beta comparison. Data calculated at 555 nm wavelength was used for comparison with satellite measurements.

The K value is measured by the a-Beta, TACCS, and AC-9 in the 532 nm wavelength. The K value is empirically derived using the Kirk relationship (Kirk, 1994). In a case study of turbid waters, Kirk represents a solid dependence of vertical attenuation for downward irradiance on absorption and scattering as:

$$K_d = (a^2 + 0.245ab)^{1/2}, \qquad (9)$$

A K value for the AC-9 was established using the a and b measurements at the 532 wavelength. In Kirk's results the direct relationship between K to the backscattering and absorption coefficients holds in waters where the b:a ratio is high. The waters in the Mississippi Bight region are also characterized by a similarly high b:a ratio.

The Secchi disk depth (z_{sd}) observed is compared to the c value from the AC-9 and the K value from the a-Beta. The 4.0/(c+K) model was used to derive vertical visibility values using c from the AC-9 and K from the a-Beta.

The horizontal sighting (R) of targets was conducted at a depth of approximately 3 meters. Targets included 20 inch black and gray spheres and a black disk. In contrast to a white Secchi disk, an all-black target (black body) reflects no light and is seen as a silhouette. The inherent contrast is –1 and sighting range depends only on the attenuation coefficients for the water and not the ambient light or reflectance coefficient. The observed horizontal distance of the target was compared to the range

values produced by using the 4.8/c model, the 4.4/c model and the beam attenuation coefficient at the 555 nm wavelength averaged over 3 meters.

V. RESULTS

A. INSTRUMENT SELECTION

The in-situ data collected from the MoDiV experiment was analyzed graphically for variability in the different instrument measurements. There are many hydro-optical instruments that objectively quantify the optical properties of the water medium. Deciding on which instrument to compare with the satellite is necessary for accurate comparisons. It is also crucial to determine the feasibility of using this instrument in the Naval Research aspect for 'through the sensor' (TTS) operational use. Due to the monetary constraints facing research and military programs, it is important to have an instrument to collect pertinent data that can be easily implemented in or with an existing naval system, such as being attached to a UAV or diver for data collection during operations.

All available instruments as listed in Table 1 were easily deployed from a small ship platform. Figure 6 is an example of the consistent performance of the AC-9 compared to the c-beta in measuring IOP's of Mississippi Bight waters. In all instances over the three-day study the data from the AC-9 was well behaved. The c-Beta showed a large increase in the attenuation coefficient at approximately 4.3 meters in every profile. A linear fit for each data set was done to show the trend of the AC-9 verses the c-Beta and the comparison of the two wavelengths on the AC-9. Because of this small variation, the 523 nm wavelength can also be used for a direct comparison with the SeaWiFS band 4, the 555 nm wavelength.

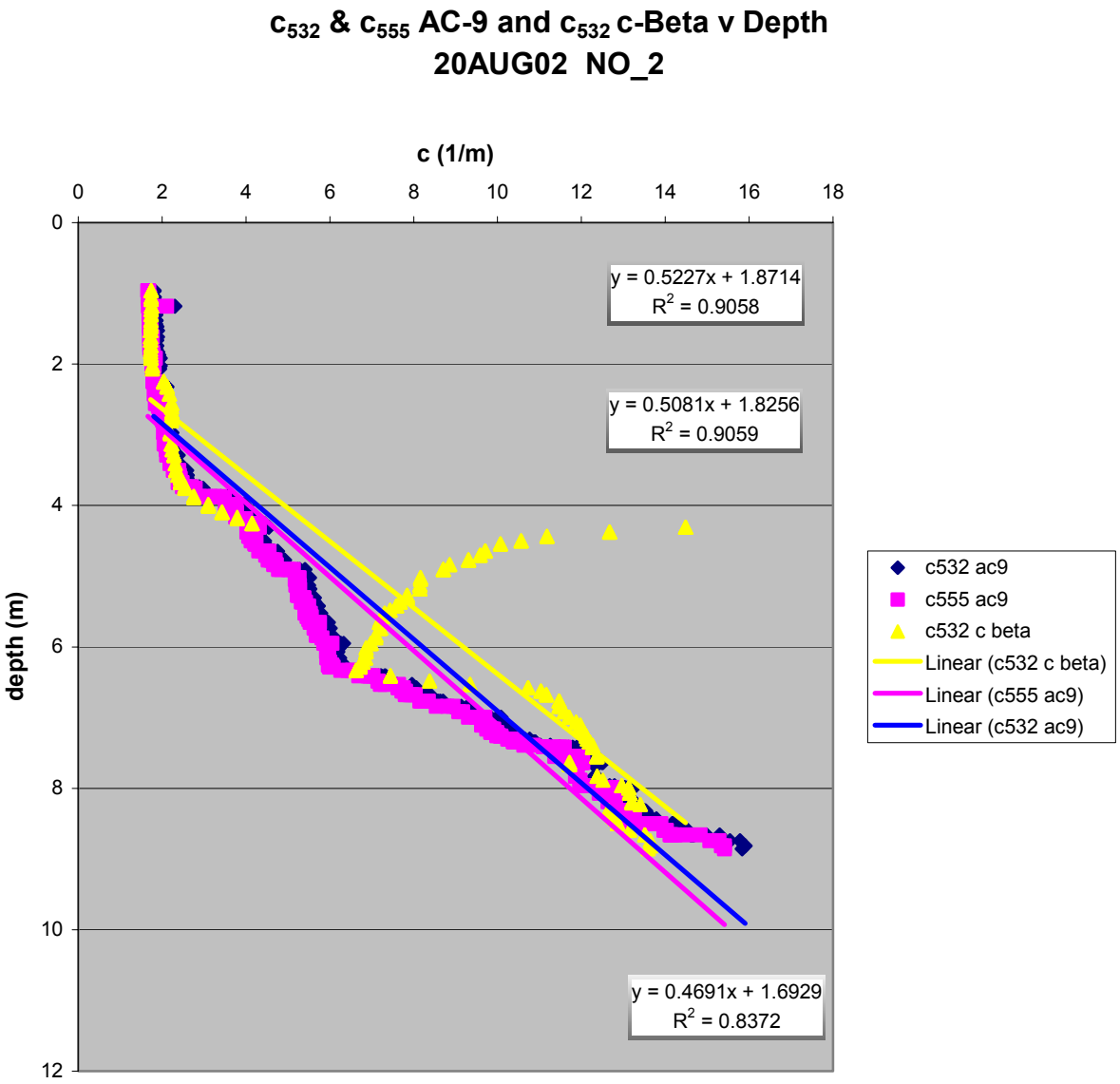

Figure 6: Plot of c vs. depth for 20AUG02 2nd drop showing the AC-9 measurements (pink at the 555 nm wavelength and blue at the 532 nm wavelength) compared to the c-beta measurements (yellow line, 532 nm wavelength.)

The AC-9 can be used to derive a K value using a relationship in equation 6. Figure 7 shows the relationship between the diffuse attenuation coefficients and the AC-9

derived values and the a-Beta measurements during the MoDiV experiment on 20 August 2002. The empirical solution of K using the AC-9 did not show data that was consistent with known K values for this type of water regime. The a-beta and TACCS instruments produced values that were consistent with average K values for turbid waters. The calculated K values are approximately one tenth the value of the a-Beta measurement. Average K values measured in turbid waters usually range from 0.1 m^{-1} to 0.8 m^{-1}. (Holmes 1970).

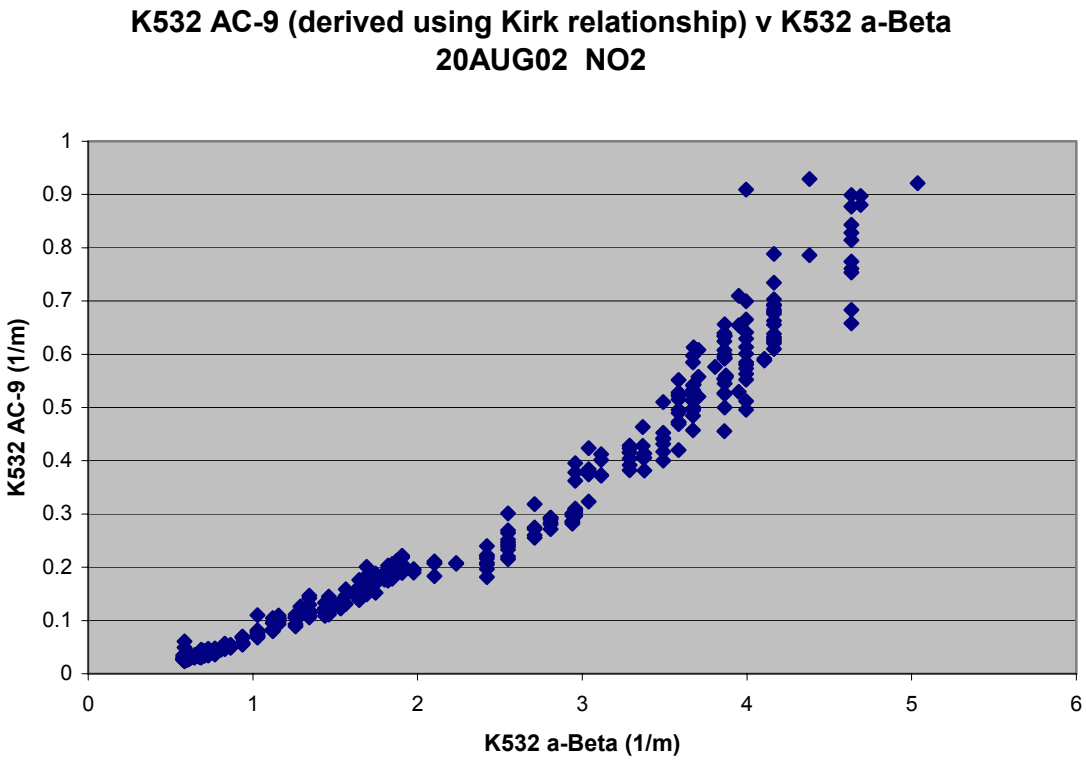

Figure 7: Comparative plot of the K 532 derived using the Kirk relationship and the K 532 values from the a-Beta instruments on 20 August 2002.

Table 2 presents a summary of the K values from the AC-9, a-Beta and TACCS instruments. When calculated, the K 532 nm wavelength for the AC-9 resulted in values inconsistent with the TACCS and a-beta instruments. The

TACCS measurement only extends to 2.75 meters in the water column, which is just above the diver's sighting depth. For these reasons the a-beta instrument was used for the satellite comparison of the beam attenuation coefficient.

Table 2: Summary of averaged K 532 values from instruments and sensor.

	K532 AC-9	K532 a-Beta	K532 TACCS	K532 SeaWiFS
19AUG02	.042	.307	.280	.314
20AUG02	.033	.626	.290	.134
21AUG02	.046	.511	.304	.160

B. VERTICAL AND HORIZONTAL VISIBILITY INSITU OBSERVATIONS

Figure 8 shows the relationship between the observed Secchi disk vertical visibility and the derived vertical visibility using the AC-9 and a-Beta for the beam attenuation and diffuse attenuation coefficients respectively. This plot shows the vertical visibility during the three days of the experiment and using the selected instruments for the c and K measurements, calculates a vertical visibility.

The derivation of the vertical visibility utilized the 4.0/(c+K) model, which is also used by APS when calculating vertical visibility from SeaWiFS. Secchi disk observations and derived vertical visibility measurements produced a strong correlation coefficient of r=0.908 but with a slope very different from 1.

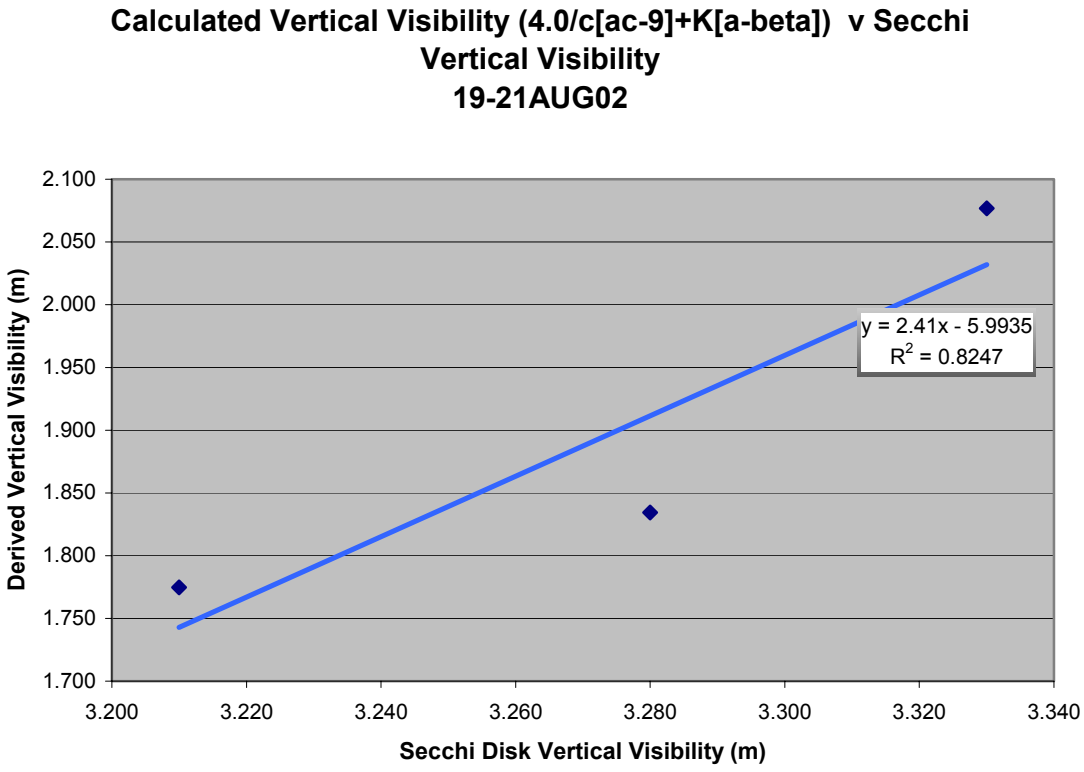

Figure 8: Correlation between Secchi Disk and derived vertical visibility using 4.0/(c+K) where c and K measurements were 5 m averages from the AC-9 and a-Beta respectively.

The focus of this thesis tries to evaluate bulk underwater visibility analysis. The diver's visibility report may not match that of the in-water instrument derivation because of the view direction or variable contrast of the target. The contrast ratio for the Secchi disk in this case was assumed to be uniform and the sun's zenith angle was assumed to be at solar noon. With these assumptions the simple models can be used for a direct comparison to the satellite products.

Horizontal visibility sighted by the divers over the three-day period yielded an average visibility of 2.46 meters at approximately 3 meters depth. Figure 9 shows an

underwater photograph of what the divers were observing. The image shows that these waters provide excellent study of the turbid water regime. The horizontal distance from the black disk is approximately 1 meter at a depth of 3 meters. The target disappeared as the diver moved further away.

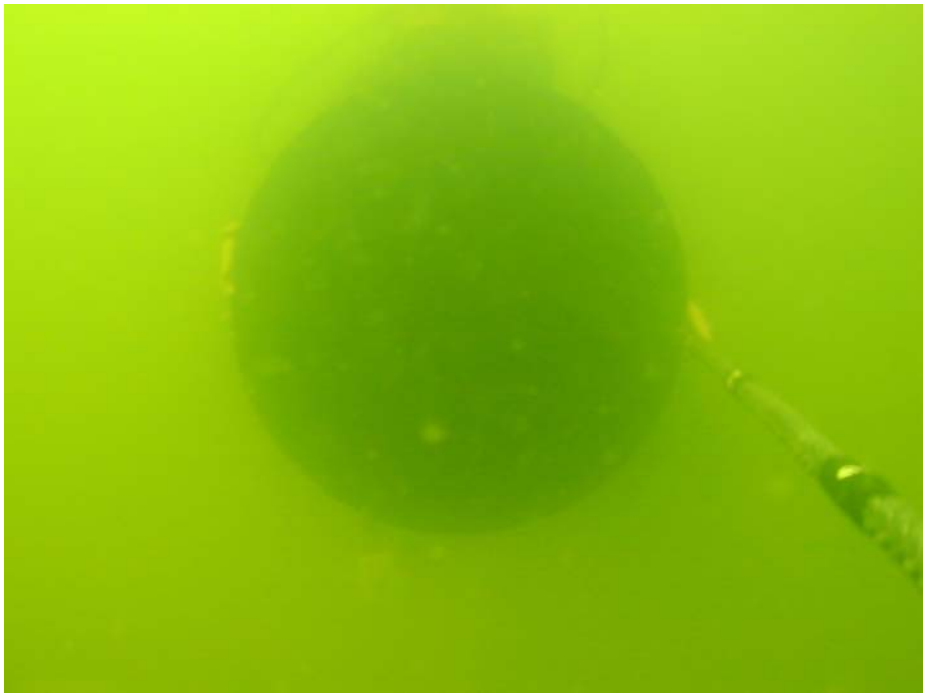

Figure 9: Diver view of a flat black target, horizontal distance of 1 meter from the target and at a depth of 3 m.

Table 3 provides the average visibilities at this depth over the three-day experiment. Based on these sightings and the 3-meter c values from the AC-9, the average contrast constant in the 1/c (inverse c) model is 4.4.

Table 3: Three-day summary of average horizontal visibility from the divers at ($30°5.5'N, 88°52.5'W$) during the MoDiV experiment.

	Visibility at 3m depth
19 Aug	2.67 m
20 Aug	2.01 m
21 Aug	2.71 m

Figure 10 illustrates the horizontal visual range using the 4.4 and 4.8 constants verses the horizontal visibility of the divers. Using a smaller contrast constant in this case matches the one to one ratio with the diver's observations.

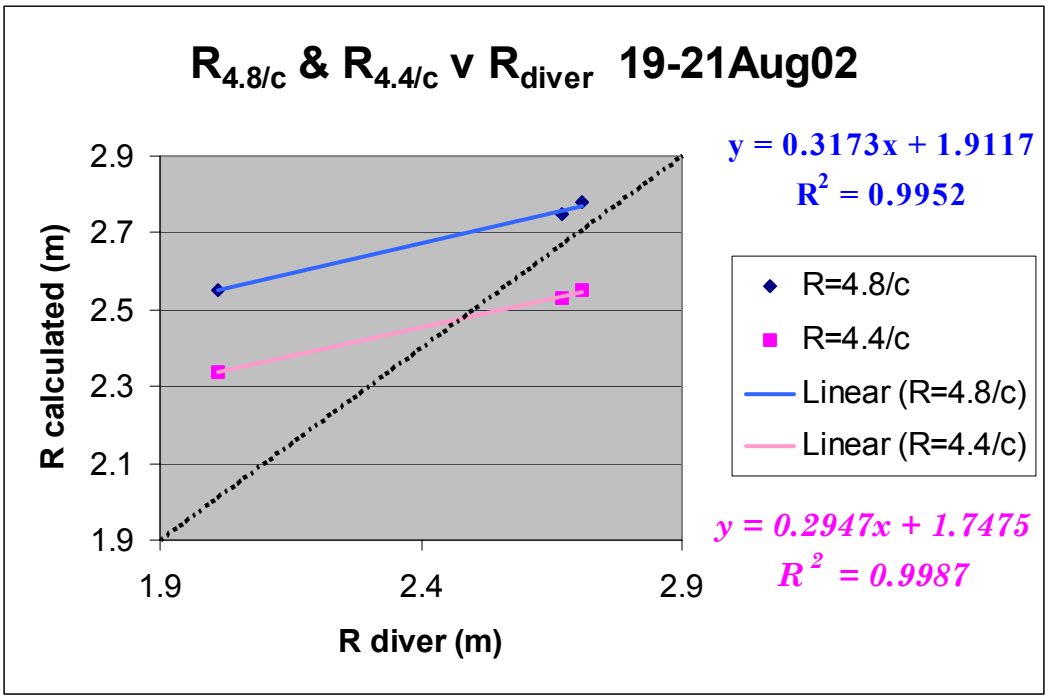

Figure 10: Correlation between contrast values for horizontal visibility and diver sightings.

C. ATMOSPHERIC ASSESSMENT

All AOT observations for 19-21 August 2002 within the temporal frame of the experiment indicated no significant impact of the atmosphere AOT. Figure 11 provides the AERONET data for 20 August. Here it can be seen that in the green portion of the spectrum used in this study the optical thickness is approximately 0.27 (units) over the Stennis Space Center Station. The weather for the day included clear skies with altocumulus passing clouds. It can be seen from Figure 11 that there are times during 20 August 2002 that have no data which indicates complete cloud coverage.

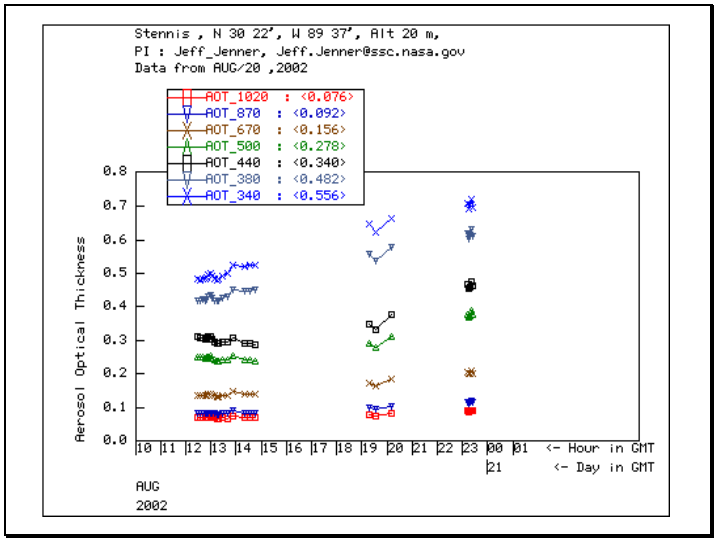

Figure 11: AERONET data for 20 August 2002.

D. SATELLITE COMPARISONS

The comparison technique was taken from the perspective of an operational METOC officer providing an estimate of horizontal (or vertical) visibility or a

particular latitude and longitude over the period of one day. Using the best satellite image available over the course of the experiment, the process of evaluating the validity of the image starts with the true color image. Figure 12 is the APS quick browse true color image. It can been seen in the area marked by the outlined yellow circle ($(30^{\circ}5.5'N, 88^{\circ}52.5'W)$), there are clear skies in the area of interest.

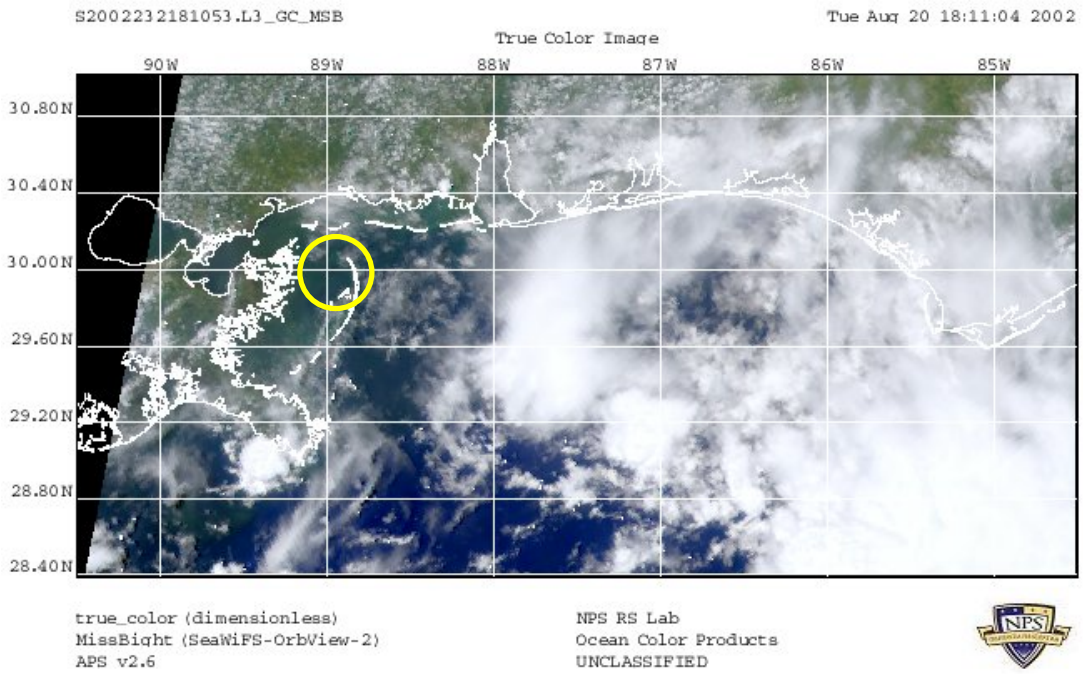

Figure 12: APS true color browse image for 20AUG2002 showing a near nadir view and clear skies over the area of interest (yellow circle).

Statistics from this area of interest as indicated by the yellow circle, were calculated for each SeaWiFS product using SEADAS. A histogram plot of each APS image with the highlighted area of interest was created to evaluate average values for the products. The histogram plot included a mean value, standard deviation and the percentage of points selected verses points used. Because

the area of interest was small and due to cloud coverage, the percentage points selected was not high. To make a concise comparison, the satellite pass for 20 August 2002 (Julian date of 232) will be used to estimate:

- the beam attenuation coefficient at the 555 nm wavelength using Carder and Arnone's algorithm,
- K at the 532 nm wavelength,
- horizontal visibility (utilizing the $4.8/c_{Carder}$ model)
- vertical visibility (using the $4.0/c_{Carder}+K$ algorithm).

1. Comparison of Beam Attenuation Coefficient 'c'

Figure 13 shows a histogram plot of APS processed SeaWiFS data using Carder's algorithm for beam attenuation at the 555 nm wavelength on 20 August 2002. All points in the highlighted area of interest were sampled for the c at 555 nm for Carder and Arnone.

Figure 14 provides a view of APS processed SeaWiFS data using Carder's algorithm for beam attenuation at the 555 nm wavelength on 20 August 2002. The beam attenuation coefficient as measured by Carder is 0.6002 m^{-1} and a standard deviation (SD) of 0.1831. Arnone's algorithm measures c as 0.8178 m^{-1} and SD of 0.3749. The average 3 meter measured value from the AC-9 on this day yielded a value of 1.88 m^{-1}. The difference in the beam attenuation coefficient values may be due to the possibility that this algorithm does not handle turbid waters as well as the clear oceans.

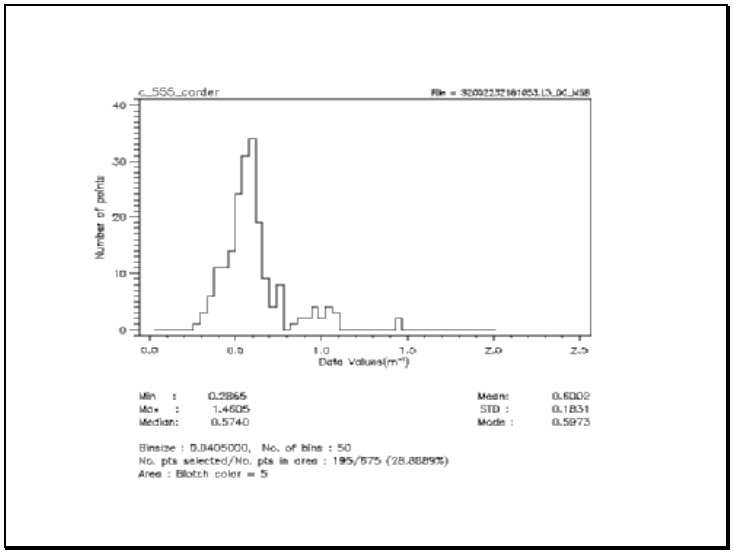

Figure 13: Histogram plot of APS processed data for the 555 nm beam attenuation coefficient on 20 August 2002.

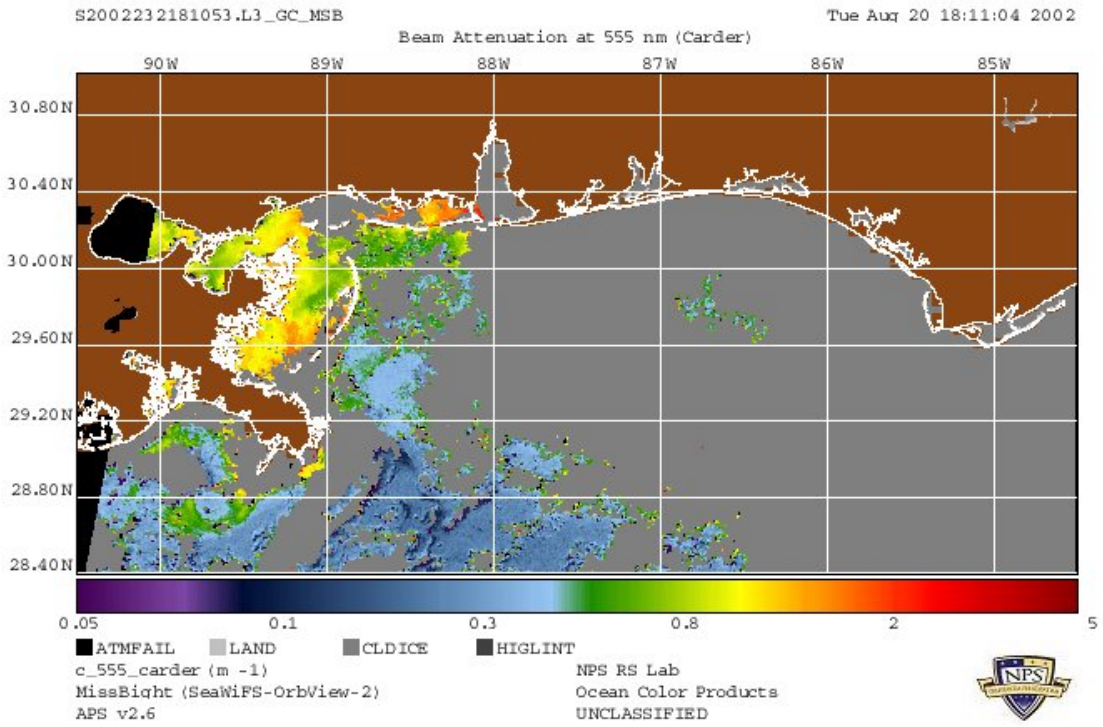

Figure 14: APS browse image of Carder's c at the 555 nm wavelength for 20 August 2002.

2. Comparison of Diffuse Attenuation Coefficient 'K'

Figure 15 shows the APS browse image of the diffuse attenuation coefficient values at the 532 nm wavelength for 20 August 2002. From the histogram plot of the area of interest for the MoDiV experiment, the mean value of the K 532 nm wavelength product from SeaWiFS for this area of interest was 0.134 m^{-1} with a standard deviation of 0.0469. Twenty-nine percent of the sampled values yielded this result. The measured value of K from the a-beta for this day was 0.626 m^{-1}, averaged over a depth of 3 meters. The variable cloud coverage lends to the large variability in the surface values and satellite values of the diffuse attenuation coefficient.

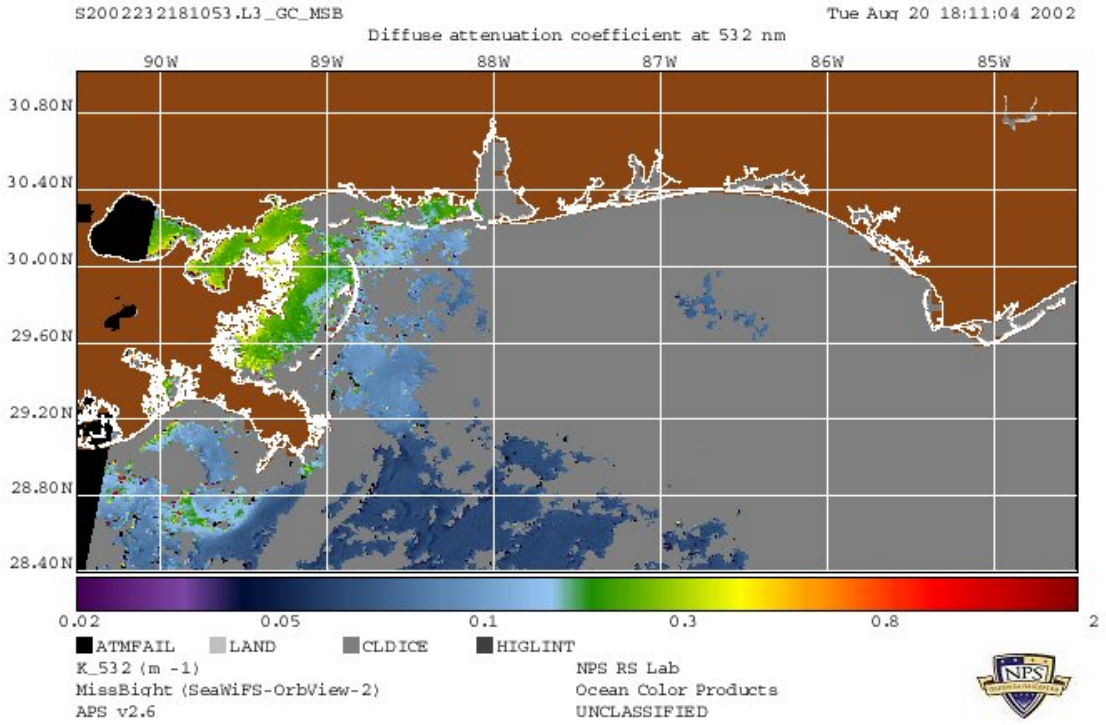

Figure 15: K at the 532 nm wavelength from APS, 20 August 2002.

3. Comparison of Vertical and Horizontal Visibilities

Figure 16 shows the vertical visibility produced by APS' quick browse feature for 20 August 2002. The current version of APS uses Carder's algorithm for c in the horizontal and vertical visibility models. The observed vertical visibility was measured at 3.28 meters by the Secchi disk. A closer fit to the observed vertical visibility is found using the beam attenuation coefficient calculated from Arnone. Arnone's algorithm handles the scattering and absorption coefficients directly and therefore when used in turbid water areas produces a value closer to the observed visibilities.

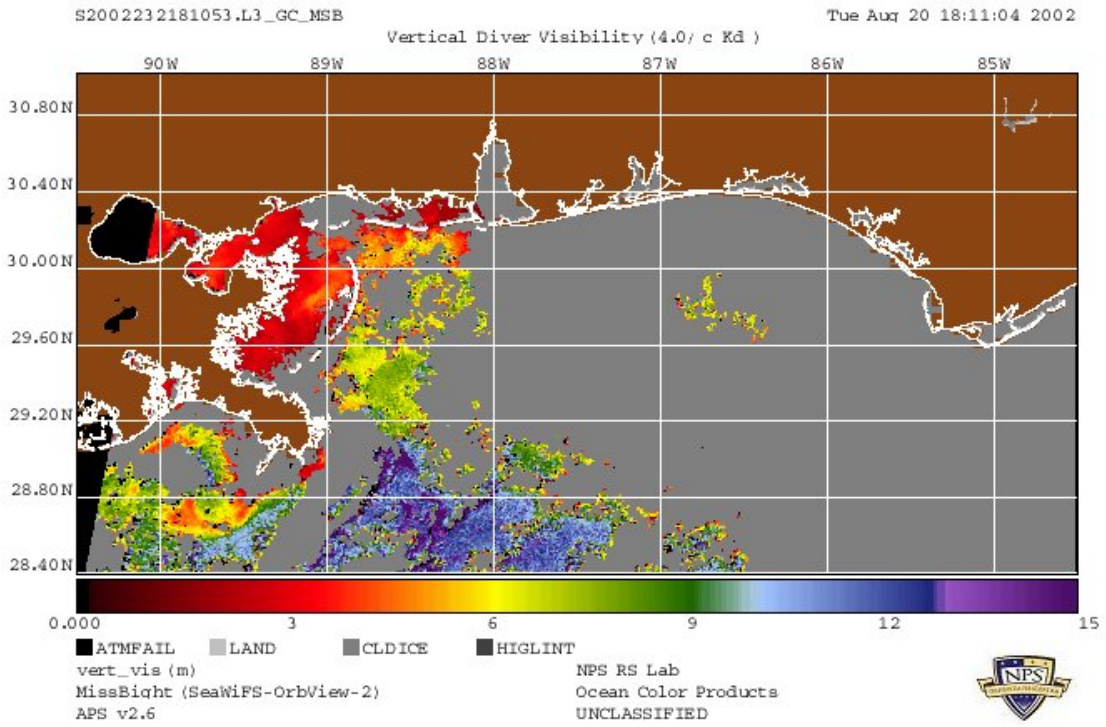

Figure 16: Quick browse image of Vertical Visibility on 20 August 2002 from APS.

Table 4 provides a summary of the value of c from SeaWiFS the standard deviation and percentage of points sampled for the area of interest. It also includes the values calculated using Arnone's algorithm for the beam attenuation coefficient at the 555 nm wavelength.

Table 4: Summary of vertical visibility using Carder and Arnone's beam attenuation coefficient algorithms.

Vert. Vis. Carder: 5.69m	Vert. Vis. Arnone: 4.58m
SD = 1.223 Percentage of points Sampled = 29%	SD = 2.223 Percentage of points Sampled = 29%

Figure 17 shows the APS browse image for the representation of horizontal visibility on 20 August 2002. The observed value of horizontal visibility was 2.01 meters from the diver observations. Using Arnone's calculation of the beam attenuation coefficient yields a higher horizontal visibility, although still significantly smaller than the observed value. Atmospheric contamination such as cirrus clouds, coupled with the algorithm's weaknesses in turbid water regimes could be causes that produced the higher than observed product values.

Table 5 summarizes the horizontal visibility values from the satellite sensor. Utilizing the same highlighted area of interest, the values of horizontal visibility from SeaWiFS were obtained (using Carder and Arnone's algorithm for c). The mean value and standard deviation were found using a histogram plot created in SEADAS for 20 August 2002.

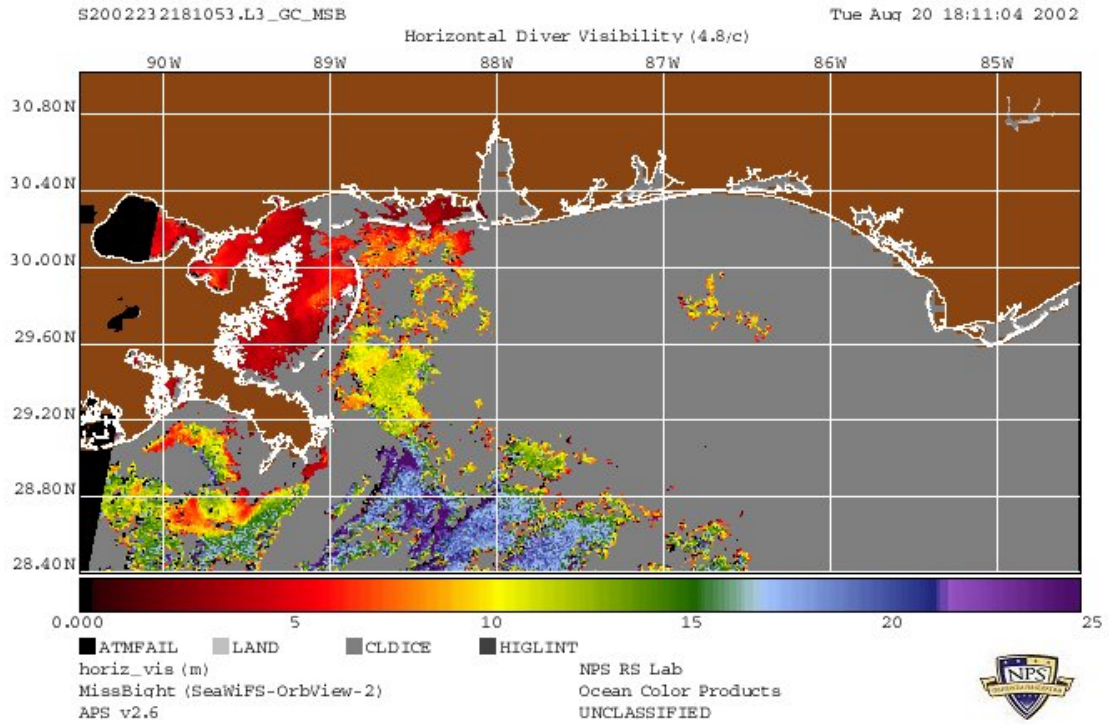

Figure 17: August 20 2002 APS reprocessed image for horizontal visibility.

Table 5: SEADAS histogram summary of horizontal for beam attenuation on 20 August 2002.visibility using the Carder and Arnone algorithms

Horiz. Vis. Carder = 7.677	Horiz. Vis. Arnone = 6.77
SD = 1.56 Percentage of points Sampled = 23%	SD = 3.16 Percentage of points Sampled = 26%

a. Composite Images of Horizontal Visibility

For Naval planning purposes detailed visibility may be required for the entire area of operations. Composite imagery can fill the gap of clouded or unprocessed data from a single pass. Figure 18, a daily composite APS image, and Figure 19, a weekly composite APS image show the large-scale view of horizontal visibility in the Mississippi Bight Region. The horizontal visibility

values for the daily (August 20, 2002) and weekly (August 14-20 2002) composites provide estimates for large-scale representations of visibility but offer the same increased values of horizontal and vertical visibility as seen in Figures 16 and 17. Because there was only one SeaWiFS pass over the Mississippi Bight region on 20 August 2002, the daily composite in Figure 18 is identical to the level-3 image in Figure 17.

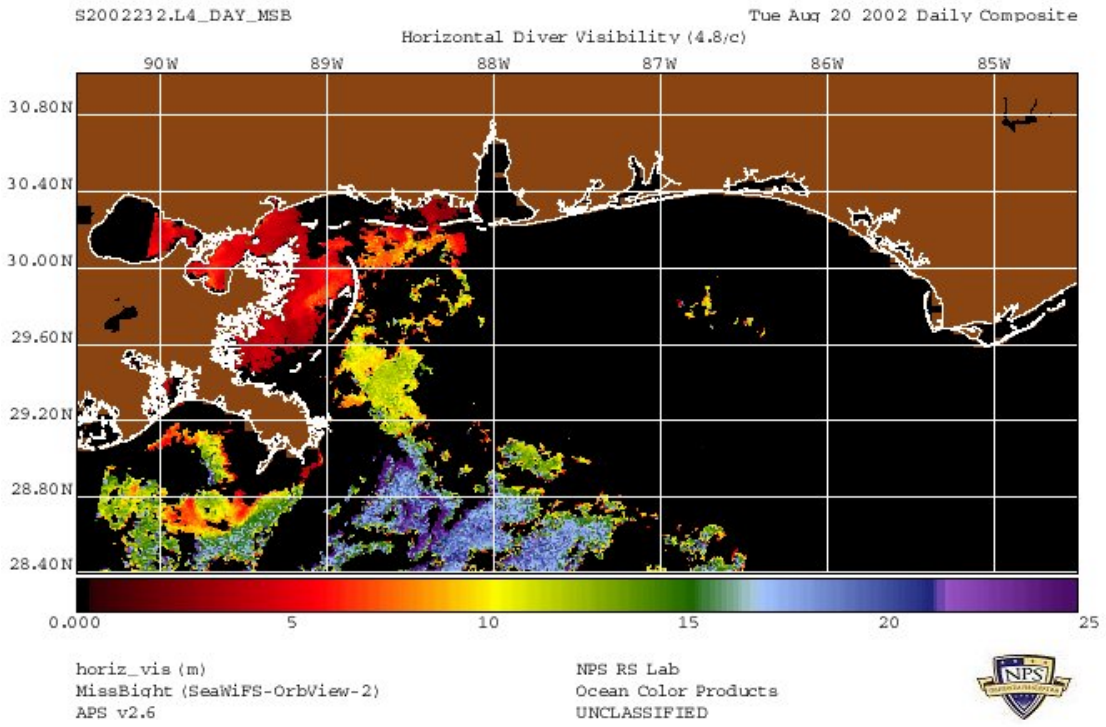

Figure 18: APS daily composite of horizontal visibility for 20 August 2002.

Level-4 weekly composite imagery may not fill all the gaps from cloud covered or unprocessed data areas. As in Figure 19, there are small areas that have no representation of horizontal visibility.

Imagery that is composited from satellite passes over an entire month offer the most comprehensive view of a region of interest. Figure 20 shows the composite

horizontal visibility for July 2002. The August composite imagery showed as many gaps due to cloud coverage as the weekly composite of Figure 19. Monthly reprocessed imagery can serve as climatic data for seasonal estimations of horizontal visibility. All values of horizontal and vertical visibility in the browse imagery for one pass are consistent with the weekly and monthly composites for the area of interest studied.

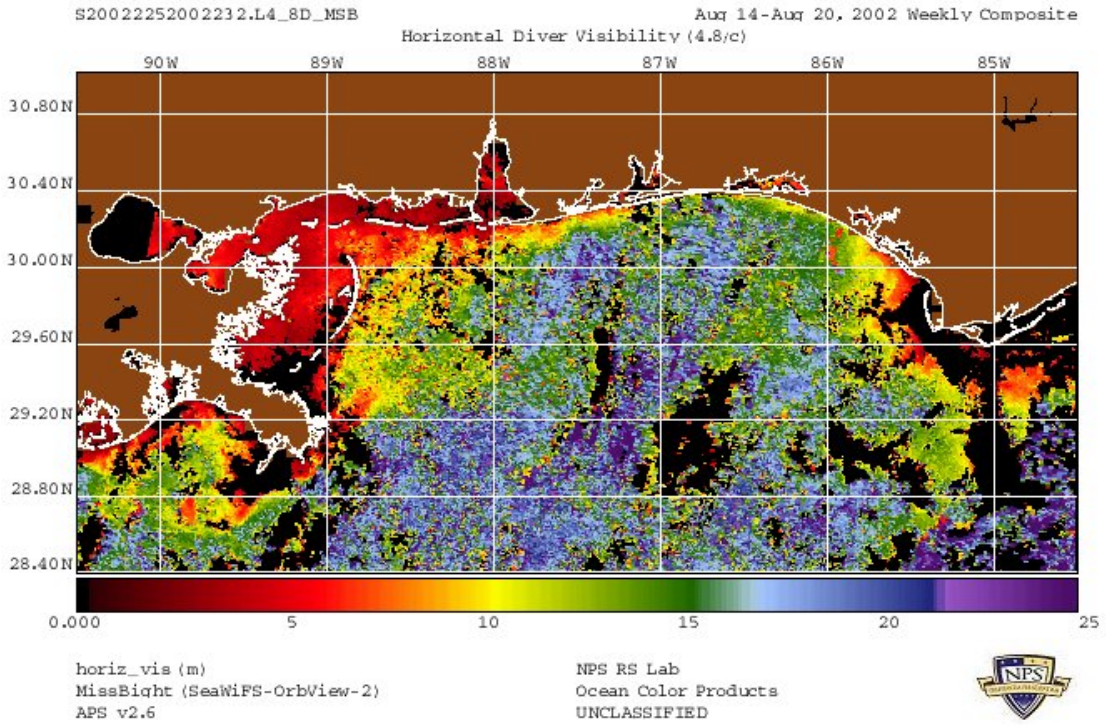

Figure 19: Weekly Composite of horizontal visibility from APS for 14-20 August 2002.

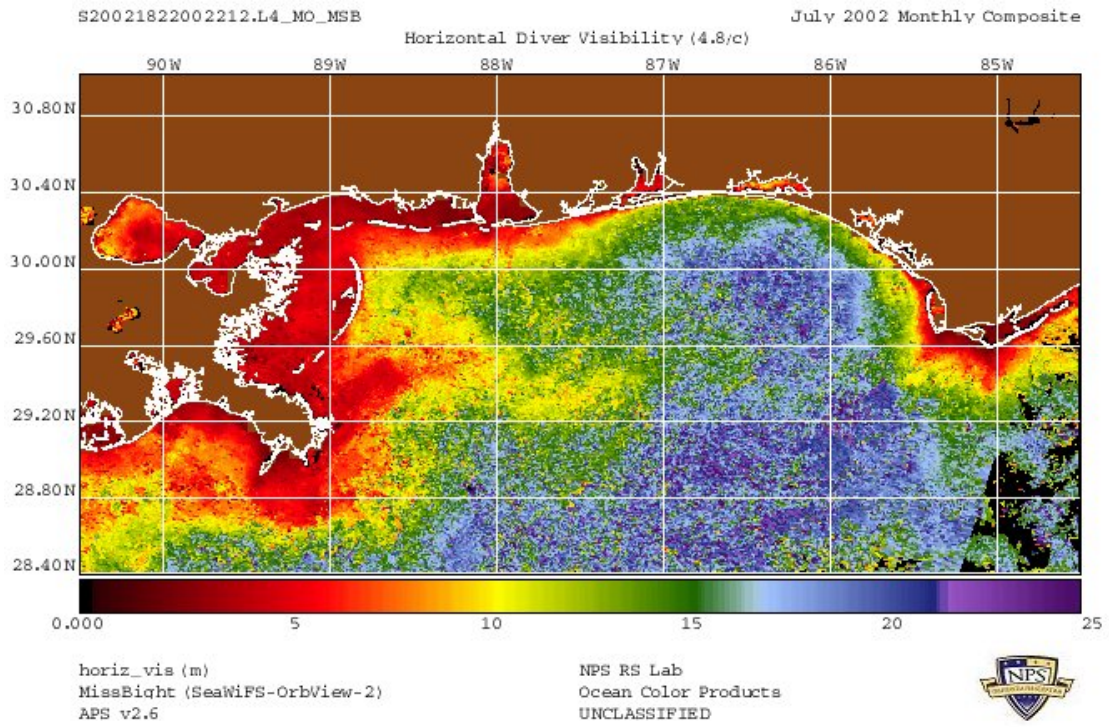

Figure 20: Horizontal visibility monthly composite from APS for July 2002.

VI. CONCLUSIONS & RECOMMENDATIONS

A. CONCLUSIONS

The objective of this thesis was to assess the study techniques for validation of visibility algorithms in turbid waters. In-situ comparison of measurements proved more successful then the satellite comparison to actual diver reports.

There were strong correlations between the diver sightings and the calculated vertical and horizontal visibilities using the models studied. The two instruments, the AC-9 and a-Beta, proved successful in verifying the use of the simple visibility models for general estimates of how far a diver can see underwater (vertically and horizontally) without knowing specific target properties. Neither formula represented a one to one ratio to the observations, Figure 8 showed the tendency for the vertical visibility derivation from the in-situ instruments to underestimate the depth visibility value compared to the Secchi measurement. Because the white Secchi disk has different limiting contrast values in turbid water and its dependence on the structure of the ambient light field, exact vertical visibility measurements are not feasible. Error estimates ranged between 55 to 78%. However, knowing its bias in this type of water can help the user in estimating a bulk vertical visibility estimate. Error values for calculated vs observed horizontal visibility ranged from 3 to 27% using the SeaWiFS algorithm model of 4.8/c and 6 to 16% using the 4.4/c model.

The small area, one pass comparison with the satellite produced large errors for the SeaWiFS visibility products. In both cases, the horizontal and vertical visibility APS products were considerable overestimates compared to the observations. Given the probability of cloud coverage due to summertime thunderstorms in the Mississippi Bight region, the satellite-retrieved results may have been contaminated much more than expected. However consistent high visibility values in one-pass, daily, weekly and monthly values lend to a weakness in the algorithms more than cloud or atmospheric contamination affects. Knowing the geography of the operational area and the climatic oceanography, the visibility products from SeaWiFS should be interpreted with much caution. Before briefing the projected visibility on the operational area of interest, observations from divers should be compared to the satellite values before reaching a conclusion on a visibility estimate.

It is difficult to determine a visibility that is representative for the human eye because of the subjectivity associated with a diver's approximation of the visibility. There are many limitations that affect even well trained observers in determining a bulk visibility for a given location. There are many times when the perception of the human eye and the sensor measurement will not match, whether it be by an instrument in the water column or from space. The human observer reports subjective estimates of the visibility and faces many limitations when trying to determine a value for visibility. Some of those limitations are viewing angle, target contrasts, and individual eye response. It is important to educate the

observer and user of the end product (the METOC officer) on the subjective verses objective measuring techniques for estimating vertical and horizontal visibility. Providing the best estimate of visibility from instruments and knowing the limits of those measurements as well as knowing the limits of the subjective view of a human, allows for an educated description of the underwater viewing environment for the warfighter.

B. RECOMMENDATIONS

Continued validation of SeaWiFS diver visibility products is needed in order to confidently apply these algorithms operationally. It is agreed upon by NRL-SSC and it is also my recommendation that the use of this product should be on an experimental basis only. Feedback from METOC centers that download SeaWiFS data and use the APS software provides critical guidance to NRL for improvements to the algorithms.

As a result of this study, the following recommendations are suggested:

1. *A determination of which instrument is best for in-situ visibility measurements needs to be established for the Navy.* A black Secchi disk used for vertical visibility eliminates the contrast and sun angle variability associated with a white disk. The AC-9 and a-Beta package in this experiment were easily deployed from the ship platform and could also be attached to an unmanned underwater vehicle (UUV) or swimmer/diver for in situ (through the sensor) measurements.

2. *Compare satellite and insitu measurements to Navy diver observations as reported.* Visibility observations

from different areas around the world can be acquired from the Diver Reporting System (DRS) environmental information that is archived at the Naval Safety Center. The DRS is a computerized database of diver mission reports that includes detailed information about the dive operations and supporting environmental data. Environmental data consists of the depth of the dive, visibility of the water, estimated current velocity, bottom type description (if deployed to the bottom) and description of any dense marine life in the area. Access to this database allows the research community to get direct diver observations for comparison to the satellite algorithms.

3. *Diver visibility observations from DRS should be submitted to the operational centers and to the research facilities.* In the aviation community pilot reports (PIREPS) are submitted to the air station when there is variability between the pilot's observations and the reported surface visibility. Dive reports (DIVREPS) should be incorporated as feedback to METOC centers for oceanographic area of responsibility (AOR) handbook documentation and to NRL code 7333 for algorithm assessments.

Today's soldiers and sailors are not responsible for deciphering the remotely sensed information available to support their mission. As a nation we rely on their complete focus on assigned missions in their specific warfare fields for absolute success. Providing more information than necessary can overwhelm an operator to the point of distraction from the focus of the primary mission. The Meteorology and Oceanographic (METOC) Officer in the

Navy is responsible for providing the detailed information about the operator’s battle environment. It is absolutely essential that remotely sensed data be applied accurately to the mission at hand. In short, the METOC Officer must apply their scientific understanding of the environment and take initiative to recognize what is required of the operator and provide custom information that exploits their environment. Analysis of ocean optics has the potential to integrate the METOC officer in organizing efficient operations planned for the Mine Warfare/Explosive Ordinance Disposal location of mine threats, successful deployment and recovery of Mine Warfare UAVs, SPECWAR shallow water insurgency operations and Salvage-Search and Rescue operations in the coastal environment.

THIS PAGE INTENTIONALLY LEFT BLANK

LIST OF REFERENCES

Avera, W., and M. Harris, 2000: Environmental Requirements for Through the Sensors Support of Mine Warfare. Naval Research Laboratory Memorandum Report 7440-00-8236, 9 pp.

Bowers, T.E., 2003: Directionally Dependent Threshold Visual Detection Range of Non-self-luminous Objects Submerged in Optically Stratified Waters. M.S. Thesis, The University of Southern Mississippi, 71 pp.

Bradley, D., and others. 2000: Oceanography and Mine Warfare. National Research Council. 100 pp.

Bukata, R.P., Jerome, J.H., Kondratyev, K.Y., and D.V. Pozdnyakov, 1995: *Optical Properties and Remote Sensing of Inland and Coastal Waters.* CRC Press, 362 pp.

Davies-Colley, R.J., 1988: Measuring water clarity with a black disk. *Limnol. Oceanogr.*, **33**(4, part 1), 616-623.

Duntley, S.Q., 1963: Light in the sea. *J. Opt. Soc. Am.,* **53**, 214-233.

Duntley, S.Q., 1952: The visibility of submerged objects. Office of Naval Research. N5ori-07831 and N5ori-07864. Bureau of Ships. Nobs-50378.

Gordon, H.R., and A.W. Wouters, 1978: Some relationships between secchi depth and inherent optical properties of natural waters. *Appl. Optics.* **17**, 21 33 – 21 3343.

Hojerslev, N.K., 1986: Visibility of the sea with spectral reference to the secchi disk. *SPIE Ocean Optics VIII,* **637**, 294-305.

Hydro-Optics, Biology and Instrumentation Laboratory. Product Listing. http://www.hobilabs.com/products March 2003.

Holmes, R.W., 1971: The secchi disk in turbid coastal waters. *Limnol. Oceanogr.,* **15**, 5 688 –5 694.

Jugan, L., 2002: Modeling Diver Visibility (MoDiV): A Validation of Present Modelling Efforts. Exercise Plan for the Naval Research Laboratory. 14 pp.

Kirk, J.T.O., 1994: Characteristics of the light field in highly turbid waters: A Monte Carlo study. *Limnol. Oceanogr.*, **39**, 3 702 -3 706.

Levin, I., Desa, Eh., Desa, El., Suresh, T., and T. Radomyslskaia, 1999: Can the secchi depth measurements be used for determination of water inherent optical properties. National Institute of Oceanography, Dona Paula, India. 7 pp.

Levin, I.M., 1980: Theory of the white disk. *Atm. and Ocean Phys.*, **16**, 9 678 -9 683.

Maffione, R.A., 2001: Evolution and revolution in Measuring ocean optical properties. *Oceanography,* **14**, 3 9 -3 14.

Martinolich, P., 2002: APS User's Guide Version 2.6. Neptune Sciences.

Mobley, C.D., 1994: *Light and Water Radiative Transfer in Natural Waters.* Academic Press, 592 pp.

Nowell, A., and others. 1997: Oceanography and Naval Special Warfare Opportunities and Challenges. National Research Council. 87 pp.

Prasad, K.S., Bernstein, R.L., Kahru, M., and B.G. Mitchell, 1998: Ocean color algorithms for estimating water clarity (Secchi depth) from SeaWiFS. *J. Adv. Mar. Sci. Tech. Soci.*, **4**, 2 301 -2 306.

Preisendorfer, R.W., 1986: Eyeball optics of natural waters: Secchi disk science. NOAA Tech. Memo. ERL PMEL-67, 89 pp.

Preisendorfer, R.W., 1976: *Hydrologic Optics*. Vol 1. U.S. Department of Commerce, 218 pp.

Satlantic. Product Listing. http://www.satlantic.com March 2003.

Spinrad, R.W., Carder, K.L., and M.J. Perry, 1994: *Ocean Optics*. Oxford University Press, 283 pp.

Weidemann, A., and LCDR K. Davis-Lunde, 2000: Ocean Response Coastal Analysis System. Joint Document NRL Document Number: N0001499WX20683 and CNMOC Document Number: N0001499WX20681, 5 pp.

Wetlabs. Product Listing. http://www.wetlabs.com March 2003.

Williams, J., 1968: The Meaningful Use of the Secchi Disk. Office of Naval Research NR 083-016, 13 pp.

THIS PAGE INTENTIONALLY LEFT BLANK

INITIAL DISTRIBUTION LIST

1. Defense Technical Information Center
   Ft. Belvoir, VA

2. Dudley Knox Library
   Naval Postgraduate School
   Monterey, CA

3. Chairman (Code MR)
   Department of Meteorology
   Naval Postgraduate School
   Monterey, CA

4. Chairman (Code OC)
   Department of Oceanography
   Naval Postgraduate School
   Monterey, CA

5. Professor Philip A. Durkee (Code MR)
   Naval Postgraduate School, Meteorology Department
   Monterey, CA

6. Robin Tokmakian (Code OC)
   Naval Postgraduate School, Oceanography Department
   Monterey, CA

7. Commander
   Naval Meteorology and Oceanography Command
   Stennis Space Center, MS